DOE-OSU-ER15172

Spectroscopic detection, characterization and dynamics of free radicals relevant to combustion processes

Final Technical Report

Period Covered: 11/01/2010 - 10/31/2014

Award #: DE-FG02-01ER15172

June 2015

Terry Miller

The Ohio State University

Columbus, Ohio

Contents

List of Figures

List of Tables

Summary

Combustion chemistry is enormously complex. The chemical mechanisms involve a multitude of elementary reaction steps and a comparable number of reactive intermediates, many of which are free radicals. Computer simulations based upon these mechanisms are limited by the validity of the mechanisms and the parameters characterizing the properties of the intermediates and their reactivity. Spectroscopy can provide data for sensitive and selective diagnostics to follow their reactions. Spectroscopic analysis also provides detailed parameters characterizing the properties of these intermediates. These parameters serve as experimental gold standards to benchmark predictions of these properties from large-scale, electronic structure calculations.

This work has demonstrated the unique capabilities of near-infrared cavity ringdown spectroscopy (NIR CRDS) to identify, characterize and monitor intermediates of key importance in complex chemical reactions. Our studies have focussed on the large family of organic peroxy radicals which are arguably the most important intermediates in combustion chemistry and many other reactions involving the oxidation of organic compounds. Our spectroscopic studies have shown that the NIR $\tilde{A} - \tilde{X}$ electronic spectra of the peroxy radicals allows one to differentiate among chemical species in the organic peroxy family and also determine their isomeric and conformic structure in many cases. We have clearly demonstrated this capability on saturated and unsaturated peroxy radicals and β-hydroxy peroxy radicals. In addition we have developed a unique dual wavelength CRDS apparatus specifically for the purpose of measuring absolute absorption cross section and following the reaction of chemical intermediates. The utility of the apparatus has been demonstrated by measuring the cross-section and self-reaction rate constant for ethyl peroxy.

Our recommendation for future work is to continue to develop the powerful NIR CRDS method to identify additional combustion related intermediates and other species whose spectroscopy can give us insight into the fundamental nature of chemical reactions. It is important to apply the newly developed multi-wavelength CRDS techniques to reliably measure absorption cross sections and the kinetic rate constants of additional chemical intermediates involved in combustion.

1 Program Scope

Combustion processes have been studied for many years, but the chemistry is very complex and yet to be fully understood. New fuels have introduced modifications to traditional mechanisms. Computer models typically employ hundreds of reaction steps with a comparable number of chemical intermediates. The predictions of such models are obviously limited by the dynamical and mechanistic data that are input. Spectroscopic identifications and diagnostics for the chemical intermediates in the reaction mechanisms constitute an important experimental benchmark for the models, as well as providing molecular parameters that are "gold standards" against which quantum chemistry computations of molecular properties may be judged. Our work has emphasized the spectroscopy of organic peroxy radicals which are key intermediates in combustion reactions. Our progress during the grant period is summarized by a series of publications,which are listed in Appendix I and whose findings are summarized below.

2 Program Progress

Organic peroxy radicals are known to be important in combustion processes. Moreover the dependence of reactions and mechanisms upon the nature of the organic group means that a variety of chemistry can occur. Peroxy radicals have a near infrared (NIR) $\tilde{A} - \tilde{X}$ electronic transition, which is typically well structured, so the spectra can serve to distinguish among, and monitor, radicals of different chemical formula, and even different isomers and conformers of the same chemical species. Analysis of these spectra can unambiguously determine the carrier and also provide important experimental benchmarks for state-of-the-art electronic structure calculations of open-shell chemical intermediates like the peroxy radicals. The technique of near-infrared (NIR) cavity ringdown spectroscopy (CRDS) of reactive chemical intermediates has been a mainstay in our laboratory and we have used it to investigate the $\widetilde{A}$ - $\widetilde{X}$ absorptions of simple alkyl peroxy radicals. These studies have created a database which allows structural/spectral relationships to be developed.[1] These relationships provide approximate predictions of spectral shifts for structural changes, e.g. *primary* (*pri*), *secondary* (*sec*), *tertiary* (*tert*) position of the peroxy group, length of the hydrocarbon chain, additional substitutions along the chain, etc. For the most part, these relationships have been based on the spectra of relatively small peroxy radicals, and are both isomer and conformer specific. Most fuels contain a mixture of larger hydrocarbons and we extended our studies to the spectroscopy of their combustion intermediates with the goal of determining how well CRDS can characterize complex peroxy radicals and mixtures of such radicals resulting from these larger hydrocarbons. All our work previously focused on peroxy radicals of alkanes and has now been extended to the corresponding radicals of unsaturated hydrocarbons and β-hydroxyalkyl peroxy radicals. A related area of CRDS spectral observations combine our alkyl peroxy work with investigations of two chemically closely related species, the halomethyl peroxy radicals, CH_2XO_2 (X=Cl, Br, I) and the very intriguing Criegee intermediate species, CH_2O_2. Another area of work involves the development of a practical CRDS apparatus to take advantage of the fact that for any absorption spectroscopy, such as CRDS, the observed signal intensity is linearly related to the concentration of the molecular species, in the limit of small absorption. We have constructed a dual wavelength CRDS apparatus (2λ-CRDS) capable of pulsed or CW operation to measure absorption cross-sections and rates of reactions for peroxy radical intermediates. The synergy between the spectroscopic and kinetic/analytical areas, using ethyl peroxy as an example, is well summarized in an invited book chapter.[2]

2.1 Spectroscopy of Unsaturated Peroxy Radicals

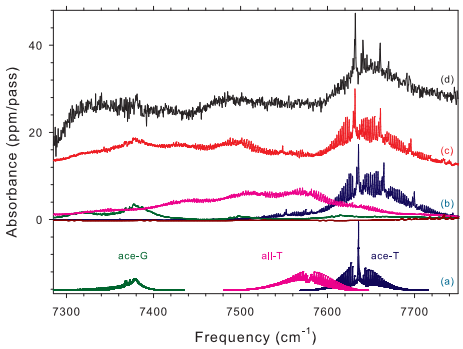

Figure 1: Comparison of simulations (a-c), based on an electronic structure calculation, with experimental spectrum (d) of propargyl peroxy in the origin region: (a) pure rotational profiles; (b) rotational profiles convolved with sequence band and torsional structure; (c) sum of the simulations in (b), where the *ace*-T and *all*-T simulations have been shifted in frequency from the calculation by -4 and -80 cm^{-1}, respectively; (d) experimental spectrum.

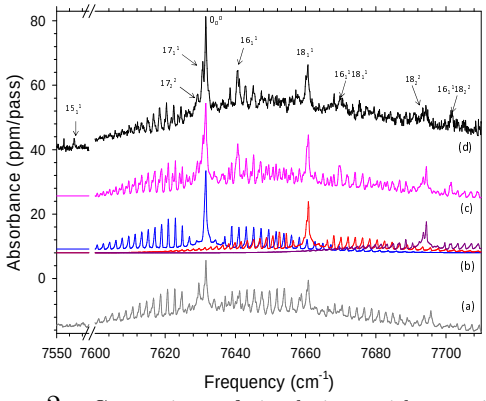

Figure 2: Comparison of simulations with experimental spectrum of propargyl peroxy in the 7550-7710 cm^{-1} region: (a) composite simulation from 1c; (b) optimized rotational profiles for band origin (blue), 18_1^1 (red), and 18_2^2 (violet) transitions, empirically shifted in frequency and weighted in intensity to match individual experimental bands; (c) sum of simulations in (b), where additional sequence bands have been added; (d) experimental spectrum. Assignments for vibrational transitions of the *ace*-T conformer of propargyl peroxy are shown above the experimental spectrum.

We have investigated the $\tilde{A} - \tilde{X}$ spectroscopy of unsaturated peroxy radicals. Species whose spectra we observed and analyzed included the peroxy radical products of allyl, propargyl, and cyclopentadienyl radical reactions with O_2. The reactants are resonantly stabilized radicals which can accumulate to relatively high concentrations in combustion and are important precursors in soot formation.[3–6] The reactions leading to the corresponding peroxy radicals may be important in the chemistry interdicting soot production.

The analysis[7] of the spectrum of propargyl peroxy was completed during this grant period and the results are shown in Figs. 1 and 2. As Fig. 3 shows one would expect two isomers, acetylenic (*ace*) and allenic (*all*). The spectra show that the *ace* isomer (T conformer) dominates although the *all* isomer (T conformer) and the *ace* isomer (G conformer) appear weakly in the spectrum.

The cyclopentadienyl peroxy (CpO_2) spectrum[8] is shown in Fig. 4. Since the Cp group is much heavier than the propargyl group, the CpO_2 spectrum does not show resolved rotational structure like the propargyl peroxy spectrum. However it does show clearly identifiable peaks that could be used to monitor the species even in the presence of other peroxy species like the HO_2 which is also generated when CpO_2 is photolytically produced starting with cyclopentadiene. Electronic structure calculations indicate that the observed CpO_2 spectrum is dominated by the G conformer but there is evidence in the spectrum for much weaker bands from the C conformer.

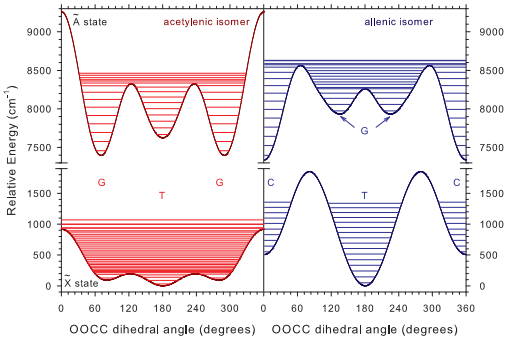

Figure 3: B3LYP potential energy surfaces of propargyl peroxy radical calculated as a function of the OOCC dihedral angle, along with calculated OOCC torsion vibrational levels. The $\tilde{A}$ state potentials have been shifted in frequency by a constant in order to match the G2 prediction for the *ace*-T conformer.

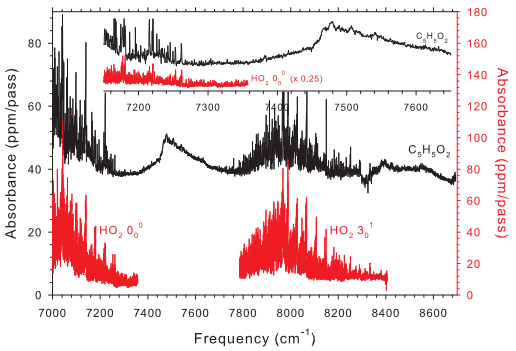

Figure 4: CRDS spectrum recorded for the $\tilde{A}-\tilde{X}$ transition of cyclopentadienyl peroxy, in comparison with that of HO_2 radical. The left and right absorbance axes correspond to the traces for cyclopentadienyl peroxy and HO_2, respectively. The cyclopentadienyl peroxy trace has been shifted +30 ppm for clarity. In the top inset, the spectrum of $C_5H_5O_2$ is compared with that of HO_2 in the band origin region.

2.2 Spectroscopy of Large Alkyl Peroxy Radicals

Following our earlier investigations of small alkyl peroxy radicals, we have recently extended[9] this work to larger species. It is well known that longer chain alkanes are important components of gasoline and diesel fuels. Nonetheless our previous CRDS spectroscopy of combustion intermediates has been limited to the $\tilde{A}-\tilde{X}$ transition of peroxy radicals with $\leq$5 carbon atoms. Recently we have extended our observations to longer chain intermediates, e.g. hexyl, heptyl, octyl, nonyl, and decyl peroxy radicals. In these experiments the peroxy radicals are formed by H atom extraction from Cl atom attack on the corresponding hydrocarbon followed by reaction with O_2. Multiple isomers of peroxy radicals can be formed as there are several unique hydrogen atoms that can be abstracted by the Cl atom. The top traces of Fig. 5 show that the spectra of all the larger peroxy radicals are dominated by two broad bands. The band near 7585 cm^{-1} is the origin band of the $\tilde{A}-\tilde{X}$ transition and about 900 cm^{-1} to the blue, there is another absorption band that results from excitation of the OO stretch vibration in the $\tilde{A}$ state.

The chemical formula for the straight chain hydrocarbons is CH_3-$(CH_2)_n$-CH_3. Clearly such species will have 6 primary sites for peroxy substitution and $2n$ sites for secondary substitution. Given that $n = 6-10$ for the hydrocarbons studied and the fact that H atom extraction by Cl is significantly favored[10] at more highly branched sites, one would expect the secondary alkyl peroxy isomers to be predominately produced. The positions of the origin bands shown in Fig. 5 all lie at $\sim$7585 cm^{-1}. Primary peroxy radical isomers typically have[9] an origin frequency that is $\lesssim$7500 cm^{-1}, so we believe that secondary peroxy radical isomers are responsible for the observed spectra. The broad lines in Fig. 5 are likely caused by the overlapping of spectral transitions of the different secondary isomers produced.

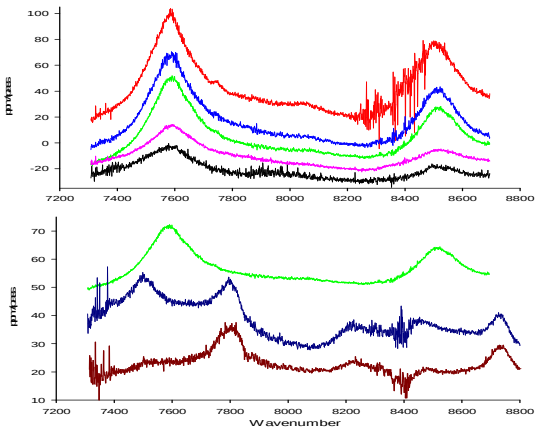

Figure 5: $\tilde{A}-\tilde{X}$ spectra of the straight chain C_6-C_{10} peroxy radicals (top). The sharp lines in the hexyl peroxy trace ($\approx$8230-8480 cm^{-1}) are due to incomplete substraction of a precursor absorption band. In the lower panels the spectrum of n-octyl (green) is compared to that of iso-octyl (blue) and iso-octyl (scarlet) peroxy after delays of 0.01 and 1 msec respectively from the photolysis laser.

Isooctane, $(CH_3)_3$C-CH_2-$CH(CH_3)_2$, is the standard for grading gasolines. The spectrum of isooctyl peroxy, also shown in Fig. 5 (bottom traces), is easily distinguished from the spectra of n-ocytl peroxy and the other straight-chain peroxy radicals. In the isooctyl peroxy spectrum there are two broad bands appearing at

7500 cm^{-1} and 7798 cm^{-1} which we assign to the origin bands of the primary and tertiary peroxy isomers, respectively, which is consistent with the origin frequencies of other primary and tertiary isomers.[1] Moreover, the long lifetime of the origin band at 7798 cm^{-1} is consistent with the long lived behavior previously observed with *tert*-butyl peroxy.[10] The additional spectral bands, assigned to the COO bend can likewise be attributed to the primary or tertiary isomer respectively, based on both their temporal behavior and frequency.

2.3 Spectroscopy of β-OH Alkyl Peroxy Radicals

β-hydroxyalkyl peroxy radicals are prototypical intermediates in the oxidation of olefins. They appear in the oxidation of ethene, propene, butene, 2-methyl butadiene (isoprene), and other larger olefins emitted in large quantities into our troposphere.[11–17] They are present in the combustion of alcohols such as ethanol, which are added to automotive fuels.[18,19] Recently we have detected the spectra of the two simplest β-hydroxy peroxy radicals, β-hydroxyethyl peroxy (β-HEP)[20,21] and β-hydroxypropyl (β-HPP).[22]

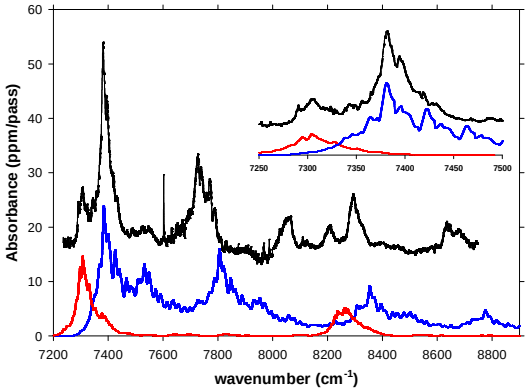

Figure 6: Spectrum of β-HEP. The experimental spectrum was obtained from 2-iodoethanol and has been digitally smoothed. Color coding is as follows: experimental spectrum (black), $G_1G_2G_3$ simulation (blue), and $G_1'G_2G_3$ simulation (red). The inset shows the experimental (black) origin region expanded along with simulations (blue and red). All simulated traces are shifted to match the experimental O_0^0 bands.

Electronic structure calculations indicate that more than 10 and 20 stable conformers should exist for β-HEP and β-HPP, respectively. However the observed room temperature CRDS spectra (see Fig. 6) for the β-HEP radical is dominated by the $G_1G_2G_3$ conformer with the spectrum of only one additional conformer visible. For β-HPP, the spectra of only 3 conformers are detected. For both radicals, the dominant spectrum is assigned to a conformer having the most favorable configuration for internal H-bonding between the hydroxy H and the terminal O of the peroxy group.

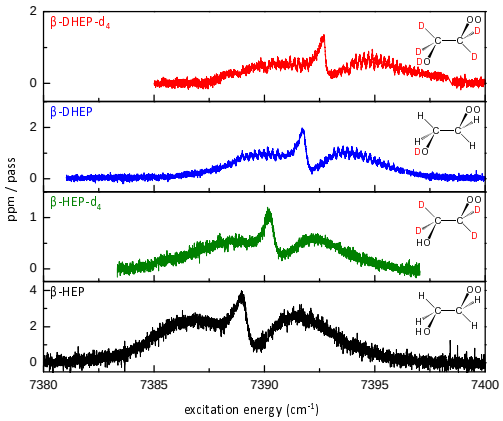

Figure 7: Experimental $\tilde{A}$–$\tilde{X}$ spectra of β-HEP isotopologues, demonstrating the differently resolved overall rotational contours. The site of deuteration is indicated in the upper right while the corresponding acronym for each isotopologue is shown in the upper left of each panel.

The importance of this H-bonding interaction is demonstrated further by the CRDS spectrum observed[21] for free jet cooled radicals. One would expect linewidths in this apparatus of $\lesssim$200 MHz. Yet Fig. 7 shows linewidths in the 1-10 GHz region which are strongly dependent on the degree of the deuteration of the radical. Such width is consistent with $\tilde{A}$ state lifetimes in the 20-60 psec range. Based upon the variation of these lifetimes with deuteration we have argued[21] that the lifetime-limiting process likely involves internal conversion from the $\tilde{A}$ state to the $\tilde{X}$ state surface, probably by coupling along the reaction path leading between HO-CH_2-CH_2-O-O and O-CH_2-CH_2-O-OH.

Based upon the hydroxy peroxy observations, we have attempted similar studies on the hydroxy alkoxy radicals which could have similar isomerization pathways leading to ·QOH radicals. This work led to a collaboration with the Butler group investigating the fragmentation dynamics of halo-substituted alkoxies.[23]

2.4 Spectroscopy Related to the Criegee Intermediate

The recent use[24] of a new gas-phase synthetic route to produce the Criegee intermediate, CH_2OO, has led to its first physical detection via mass spectrometry[25] and a surge in kinetic and related studies.[26–29]

Recently both the IR vibrational spectrum[30] in the ground state and the $\tilde{B} - \tilde{X}$ electronic spectrum[31] have been reported and there have been reports[32] of its microwave spectra. While the protocols of various workers have differed in details the basic idea, as illustrated in Fig. 8, is the same, i.e. photolysis of a CH_2I_2 precursor produces CH_2I which reacts with O_2 to release I and form CH_2O_2.

CH_2OO is isoelectronic with ozone, O_3. In the ozone absorption spectrum there is a well-known transition[33,34] from the $\tilde{X}^1A_1$ ground state to the $\tilde{a}^3A_2$ excited state known as the Wulf Band whose origin occurs at 9553 cm^{-1}. Since O_3 and CH_2OO are isoelectronic, we would expect an $\tilde{a}^3A' - \tilde{X}^1A'$ transition for CH_2O_2 analogous to the Wulf Band. Simple valence bond models argue[35,36] that the origin of the $\tilde{a}^3A' - \tilde{X}^1A'$ band in Criegee would be red shifted from the O_3 value and likewise preliminary *ab initio* calculations predicted a red shifted origin at ≈6800 cm^{-1}.

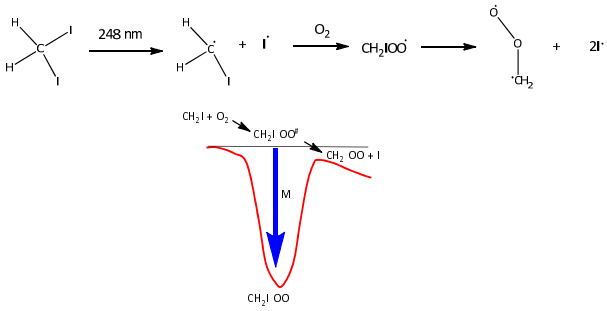

Figure 8: Proposed mechanism for the production of CH_2O_2 indicating a possible second channel producing CH_2IO_2.

We have used the synthetic procedure[29] shown in Fig. 8 and have observed the NIR spectrum shown in Figure 9. As the figure shows, this spectrum has several characteristics expected of CH_2O_2. Its apparent origin is in the NIR, just below 7000 cm^{-1}, and it clearly exhibits an O-O stretch and combination bands whose frequencies are characteristic, albeit slightly lower, than those in typical alkyl peroxy radicals. However the information available from the spectrum is limited by signal/noise as well as interference from several other species and some spectral features, e.g. the complex structure near the origin, are difficult to understand. While good electronic structure calculations exist for the $\tilde{X}^1A'$ state, there are at present no reliable calculations for the $\tilde{a}^3A'$ state that could aid the detailed assignment of the spectrum.

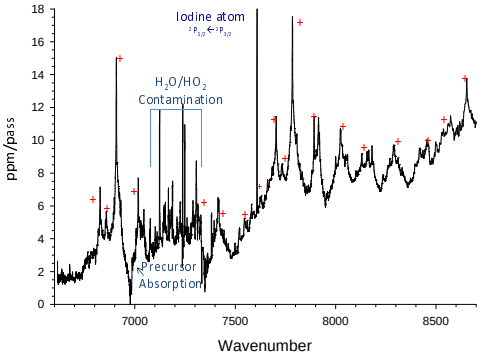

Figure 9: Spectrum obtained from 248 nm photolysis of CH_2I_2 precursor. Red plus signs denote absorption bands that belong to the spectral carrier(s) of interest.

Fig. 8 shows that another species postulated to be formed from the CH_2I_2 photolysis chemistry is CH_2IO_2. The general characteristics of the observed spectrum in Fig. 9 are also broadly consistent with assignment to CH_2IO_2, whose excited $\tilde{A}$ state likewise is somewhat difficult to calculate reliably due to the need to use a pseudo-potential for the I atom. We have therefore decided to compare the spectrum in Fig. 10 to the spectra of CH_2ClO_2 and CH_2BrO_2. These species have been generated by photolysis of CH_2ClI or CH_2BrI. (Indistinguishable spectra are also observed when CH_2Cl_2 and CH_2Br_2 respectively are photolyzed.)

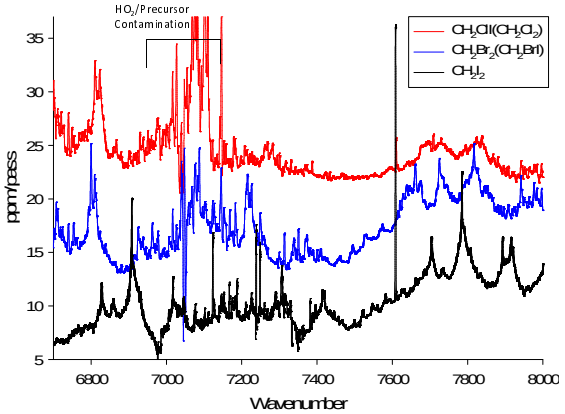

Figure 10: Red and blue traces are CRDS spectra attributed to CH_2ClO_2 and CH_2BrO_2. The bottom (black) trace is from Fig. 9.

Fig. 10 shows there is also a good deal of similarity among the spectra produced by photolyzing CH_2ClI, CH_2BrI, and CH_2I_2. However it could be argued that the spectrum resulting from CH_2I_2 shows some unique features. Other spectral evidence, e.g. rotational contours and the origin structure, also probably favors its assignment to CH_2IO_2 although numerous questions exist with this assignment.

In order to attempt to confirm the assignments on the experimental spectra to the halogenated methyl

peroxy radicals CH_2XOO(X = Cl, Br, I), we calculated the Franck-Condon spectrum for all the species based on electronic structure. Calculations are performed with Gaussian 09[37] package to obtain the molecular geometry and vibrational frequencies of the molecules. For CH_2ClOO and CH_2BrOO radicals, B3LYP/aug-cc-pVTZ level of theory and basis sets are used for the $\widetilde{X}$ state calculation while TDB3LYP/aug-cc-pVTZ level of theory and basis sets are used for the $\widetilde{A}$ state. In terms of the energy difference between the $\widetilde{X}$ and $\widetilde{A}$ states, G2 calculations are performed on both states to obtain accurate absolute electronic energies. In order to apply the G2 calculations on $\widetilde{A}$ states, the electronic configuration was obtained by permuting the HOMO and SOMO orbitals of the radicals in the initial SCF estimate. For the CH_2IOO radical, a basis set with psuedo potential, aug-cc-pVTZ-PP is combined with the B3LYP and TDB3LYP calculations on the $\widetilde{X}$ and $\widetilde{A}$ states, respectively. In addition, Richard Dawes has collaborated with us and performed a higher level electronic structure calculation on CH_2IOO radical with UCCSD(T*)-F12b/VDZ-F12 level of theory and basis set on $\widetilde{X}$ state and CASSCF(13e,12o)/VDZ-F12 of theory and basis set on $\widetilde{A}$ state. The calculated parameters use the TDB3LYP method are listed in the Table 1.

Table 1: Predicted experimental $\widetilde{A}$ state vibrations for the G conformer of CH_2IO_2·. Mode numbering follows Herzberg's notation and is based on the values of the $\widetilde{A}$ state frequencies. The number in the bracket is the $\widetilde{X}$ state torsional frequency.

Mode	Description	Experiment	TDB3LYP	CASSCF(13e,12o)
ν_{12}	OOCI torsion	109(80)	101(85)	120(82)
ν_{11}	OCI bend	238	279	270
ν_{10}	COO bend	397	398	423
ν_9	C-I stretch	508	519	539
ν_8	CH_2 rock + O-O stretch	877	847	851
ν_7	O-O stretch + C-O stretch	–	915	912
ν_6	O-O stretch + C-O stretch	1011	1043	1072
ν_5	C-H_2 torsion	–	1233	1328
ν_4	C-H_2 sway	–	1252	1359
ν_3	HCH bend	–	1457	1582
ν_2	C-H_2 symmetric stretch	–	3105	3275
ν_1	C-H_2 asymmetric stretch	–	3203	3377

Combined with the calculations above, simulations of the entire experimental spectra for the CH_2IOO· radical, are shown in Figs. 11 and 12. In these simulations, the intensities and frequencies of the torsional features are calculated based on the torsional potential with parameters from the UCCSD(T*)/CASSCF(13e,12o) calculations. For the normal modes except torsion, the intensity of the fundamentals and combination bands between these modes are obtained from an eZspectrum calculation.[38] These fundamentals as well as combination bands are labeled in the figures. The torsional feature combined with each fundamental or combination band is scaled and shifted on top of the fundamental as it was on the origin region, following the same color coding. The vibrational frequencies of the modes are fitted to match the experiment. The comparison between the experimental and calculated frequencies are listed in Table 1. The close agreement of the simulated and observed spectrum coupled with the good agreement between the calculated and experimental vibrational frequencies provide compelling evidence that the carrier of the observed spectrum

is CH_2IO_2.

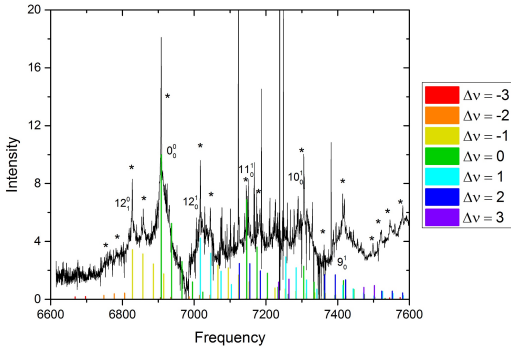

Figure 11: The Experimental and simulated spectra for all modes in the 6600cm^{-1} - 7600cm^{-1} region of the $\tilde{A}$-$\tilde{X}$ transition of $CH_2IOO\cdot$ radical

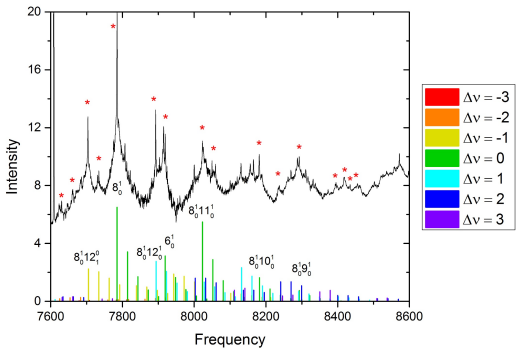

Figure 12: The Experimental and simulated spectra for all modes in the 7600cm^{-1} - 8600cm^{-1} region of the $\tilde{A}$-$\tilde{X}$ transition of $CH_2ClOO\cdot$ radical

2.5 Kinetics Related Measurements

We have constructed a dual wavelength apparatus, 2λ-CRDS, capable of measuring simultaneously two species in a reacting sample. This apparatus is illustrated in Fig. 13, and it was first used to measure[39] the peak absorption cross-section, σ_p, of $C_2H_5O_2$. This was accomplished by simultaneous absolute-intensity measurements of the $C_2H_5O_2$ and HCl CRDS spectra. This approach has been dubbed the reporter technique because using the known cross-section of the reporter molecule, HCl, its intensity measurement determines its concentration. The HCl concentration is equal to that of $C_2H_5O_2$ since HCl is formed by Cl atom abstraction of a H atom from ethane to yield C_2H_5 which is stoichiometrically converted to $C_2H_5O_2$ under the conditions of the experiment.

A cross-section measured in this fashion is both temperature and pressure dependent. However in subsequent work[40] we have simulated those dependencies to determine the electronic transition moment, μ, for the $\tilde{A}-\tilde{X}$ transition of $C_2H_5O_2$. The determination of μ allows measurements of the ethyl peroxy concentration from its CRDS absorption under a variety of conditions.

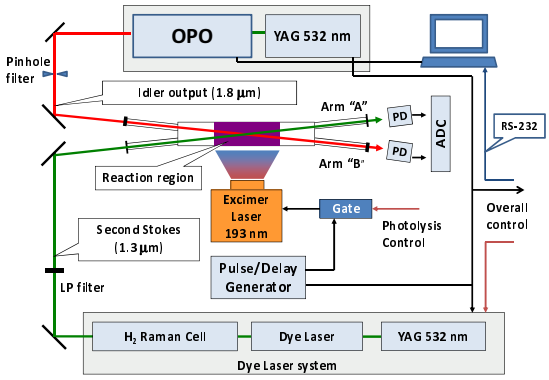

Figure 13: Schematic diagram of the 2λ-CRDS apparatus.

We have also measured[41] the rate constant for $C_2H_5O_2$ self reaction with one arm of the 2λ-CRDS apparatus utilizing a CW laser. This arrangement gives us several important capabilities. First the linewidth of the CW laser is so narrow that it is always small compared to the widths of the molecular absorption even for molecules with resolved rotational structure, thereby satisfying a necessary condition[42] for a simple, linear relationship between the CRDS signal intensity and carrier concentration. The second advantage is that because the source is continuous we can monitor the variation of concentration at a much faster repetition rate than a traditional CRDS experiment. In fact in most cases we can sample sufficiently rapidly to determine a complete kinetic decay curve for a reactive species on each shot of the photolysis laser that initiates the reaction. This approach eliminates errors, e.g. shot-to-shot variation in initial number density, common to previous methods which constructed kinetic curves combining data points at different time delays from separate photolysis laser shots. The fast repetition rate and corresponding high duty factor speeds overall data collection, allowing more signal averaging if necessary to

achieve good signal/noise.

The capabilities of the apparatus for measurement of the self-reaction rate of the ethyl peroxy radical[43] are illustrated in Fig. 14. The rapid periodic sweep of the laser frequency generates a succession of ringdown events which are displayed in panels (a) and (b). Panel (a) shows a succession of decays prior to the photolytic generation of radicals, which determines the ringdown time of the cavity in the absence of ethyl peroxy. Panel (b) shows a succession of more rapid decays shortly after the photolysis pulse and these ringdown curves determine the absorption, A, of ethyl peroxy which generates the A and A^{-1} vs. time plots shown in panels (c) and (d) respectively. In the absence of any competing removal processes, the slope of the straight line in panel (d) is k_{obs}/σ_P, in which k_{obs} is the effective reaction rate constant for the peroxy radical self-reaction, including secondary chemistry effects. Competing radical removal processes due to macroscopic flow and diffusion, do contribute in a minor way to the observed decay rate, but these effects can be easily accounted for to obtain k_{obs}.

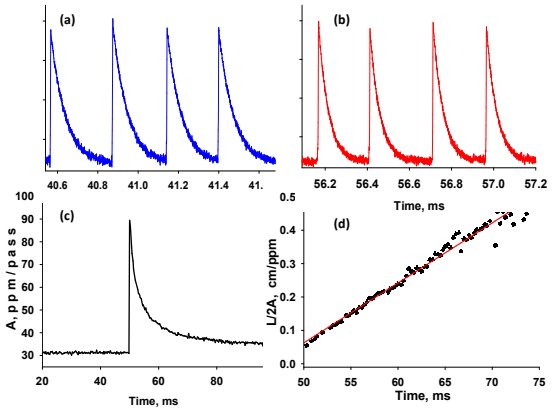

Figure 14: Spectroscopic measurements of the kinetic rate constant for $C_2H_5O_2$ self decay. Panels (a) and (b) show decay curves of the probing light without (a) and with (b) radicals present. Each light decay curve produces a single data point on the temporal absorption profile, plotted as absorption (c) and inverse absorption (d) vs. time.

The experimentally observed value for the k_{obs}/σ_P was found to be $1.827(45)\cdot10^7$ cm/s. Combination of this value with the previously published value[39] of σ_P=$5.29(20)\cdot10^{-21}$ cm^2, determines the effective value for the self-reaction[43] to be k_{obs} =$9.66(44)\cdot10^{-14}$ cm^3/s with the error largely due to the uncertainties in σ_P. The newly obtained value is consistent with most of the previously available results[41,44–49] but enjoys better precision than most of the other determinations.

3 Conclusions

This work has demonstrated the unique capabilities of NIR CRDS experiments to identify, characterize and monitor intermediates of key importance in complex chemical reactions. Our studies have focussed on the large family of peroxy radicals which are arguably the most important intermediates in combustion chemistry and many other reactions involving the oxidation of organic compounds. Our spectroscopic studies have shown that the NIR $\tilde{A}-\tilde{X}$ electronic spectra of the peroxy radicals allows one to differentiate among chemical species in the organic peroxy family and also determine their isomeric and conformic structure in many cases.

Specific family groups whose spectra was first identified include peroxy radicals formed from alkanes with 1-10 carbon atoms. We have observed the spectra of unsaturated peroxy radicals resulting from addition to allyl, propargyl, and cyclopentadienyl radicals. We have also observed the β-hydroxy peroxy radicals formed from addition of OH and O_2 to the two sides of the olefinic bond, specifically for the ethene and propene molecules. In addition we have developed a unique dual wavelength CRDS apparatus for the purpose of measuring absolute absorption cross section and following the reaction of chemical intermediates. The utility of the apparatus has been demonstrated by measuring the cross-section and self-reaction rate constant for ethyl peroxy.

References

[1] "The Structure and Spectra of Organic Peroxy Radicals," E. N. Sharp, P. Rupper, and T. A. Miller, *Phys. Chem. Chem. Phys.* **10**, 3955 (2008).

[2] "Detection and Characterization of Reactive Chemical Intermediates Using Cavity Ringdown Spectroscopy," N. Kline and T. A. Miller, in *Cavity Enhanced Spectroscopy and Sensing*, (Springer-Verlag, Berlin Heidelberg, 2014), p. Chapter 2.

[3] "Making Sure That Hydrofluorocarbons are 'Ozone Friendly'," J. S. Francisco and M. M. Maricq, *Acc. Chem. Res.* **29**, 391 (1996).

[4] "The Recombination of Propargyl Radicals: Solving the Master Equation," J. A. Miller and S. J. Klippenstein, *J. Phys. Chem. A* **105**, 7254 (2001).

[5] "The Recombination of Propargyl Radicals and Other Reactions on a C_6H_6 Potential," J. A. Miller and S. J. Klippenstein, *J. Phys. Chem. A* **107**, 7783 (2003).

[6] "On the Combustion Reactions of Hydrogen Atoms with Resonance-Stabilized Hydrocarbon Radicals," L. B. Harding, S. J. Klippenstein, and Y. Georgievskii, *J. Phys. Chem. A* **111**, 3789 (2007).

[7] "$\tilde{A} - \tilde{X}$ Absorption of Propargyl Peroxy (H-C=C-$CH_2OO\cdot$): A Cavity Ring-Down Spectroscopic and Computational Study," P. S. Thomas, N. D. Kline, and T. A. Miller, *J. Phys. Chem. A* **114**, 12437 (2010).

[8] "The $\tilde{A} - \tilde{X}$ Absorption of Cyclopentadienyl Peroxy Radical (c-$C_5H_5OO\cdot$): A Cavity Ringdown Spectroscopic and Computational Study," P. S. Thomas and T. A. Miller, *Chem. Phys. Letts.* **514**, 196 (2011).

[9] "Observation of the $\tilde{A} - \tilde{X}$ Electronic Transition of C_6-C_{10} Peroxy Radicals," N. D. Kline and T. A. Miller, *Chem. Phys. Lett.* **601**, 149 (2014).

[10] "Near-IR Cavity Ringdown Spectroscopy and Kinetics of the Isomers and Conformers of the Butyl Peroxy Radical," B. G. Glover and T. A. Miller, *J. Phys. Chem. A* **109**, 11191 (2005).

[11] "Computational Studies of Intramolecular Hydrogen Atom Transfers in the β-Hydroxyethylperoxy and β-Hydroxyethoxy Radicals," K. T. Kuwata, T. S. Dibble, E. Sliz, and E. B. Petersen, *J. Phys. Chem. A.* **111**, 5032 (2007).

[12] "Unimolecular Decomposition of β-Hydroxyethylperoxy Radicals in the HO·-Initiated Oxidation of Ethene: A Theoretical Study," S. Olivella and A. Solé, *J. Phys. Chem. A.* **108**, 11651 (2004).

[13] "Unexpected Epoxide Formation in the Gas-Phase Photooxidation of Isoprene," F. Paulot, J. D. Crounse, H. G. Kjaergaard, A. K*ü*Rten, J. M. S. Clair, J. H. Seinfeld, and P. O. Wennberg, *Science* **325**, 730 (2009).

[14] "HO_x Radical Regeneration in the Oxidation of Isoprene," J. Peeters, T. L. Nguyen, and L. Vereecken, *Phys. Chem. Chem. Phys.* **11**, 5935 (2009).

[15] "Isomer-Selective Study of the OH-Initiated Oxidation of Isoprene in the Presence of O_2 and NO: 2. The Major OH Addition Channel," B. Ghosh, A. Bugarin, B. T. Connell, and S. W. North, *J. Phys. Chem. A* **114**, 2553 (2010).

[16] "Theoretical Study of OH-O_2-Isoprene Peroxy Radicals," W. Lei, R. Zhang, W. S. McGivern, A. Derecskei-Kovacs, and S. W. North, *J. Phys. Chem. A* **105**, 471 (2001).

[17] J. G. Calvert, R. Atkinson, J. A. Kerrr, S. Madronich, G. K. Moortgart, T. J. Wallington, and G. Yarwood, *The Mechanisms of Atmospheric Oxidation of the Alkenes* (Oxford University Press, New York, 2000).

[18] "Numerical and Experimental Studies of Ethanol Flames," P. Saxena and F. A. Williams, *Proc. Combust. Inst.* **31**, 1149 (2007).

[19] "Isomer-Specific Influences on the Combustion of Reaction Intermediates in Dimethyl Ether/Propene and Ethanol/Propene Flame," J. Wang, U. Struckmeier, B. Yang, T. A. Cool, P. Osswald, K. Kohse-Höinghaus, T. Kasper, N. Hansen, and P. R. Westmoreland, *J. Phy. Chem. A* **112**, 9255 (2008).

[20] "Observation of the $\widetilde{A}-\widetilde{X}$ Electronic Transition of the β-Hydroxyethylperoxy Radical," R. Chhantyal-Pun, N. D. Kline, P. S. Thomas, and T. A. Miller, *J. Phys. Chem. Lett.* **1**, 1846 (2010).

[21] "Spectroscopic Studies of the $\tilde{A}-\tilde{X}$ Electronic Spectrum of the β-Hydroxyethylperoxy Radical: Structure and Dynamics," M.-W. Chen, G. M. P. Just, T. Codd, and T. A. Miller, *J. Chem. Phys.* **135**, 184304 (2011).

[22] "Analysis of the $\tilde{A}-\tilde{X}$ Electronic Tranistion of the 2,1-Hydroxypropylperoxy Radical Uisng Cavity Ringdown Spectroscopy," N. D. Kline and T. A. Miller, *Chem. Phys. Letts.* **530**, 16 (2012).

[23] "Imaging and Scattering Studies of the Unimolecular Dissociation of the $BrCH_2CH_2O$ Radical from $BrCH_2CH_2ONO$ Photolysis at 351 nm," L. Wang, C.-C. Lam, R. Chhantyal-Pun, M. D. Brynteson, L. J. Butler, and T. A. Miller, *J. Phys. Chem. A* **118**, 404 (2014).

[24] "Mechanism of Ozonolysis," R. Criegee, *Angew. Chem. Int. Ed.* **14**, 745 (1975).

[25] "Direct Observation of the Gas-Phase Criegee Intermediate (CH_2OO)," C. A. Taatjes, G. Meloni, T. M. Selby, A. J. Trevitt, D. L. Osborn, C. J. Percival, and D. E. Shallcross, *J. Am. Chem. Soc.* **130**, 1183 (2008).

[26] "Direct Measurements of Conformer-Dependent Reactivity of the Criegee Intermediate CH_3CHOO," C. A. Taatjes, O. Welz, A. J. Eskola, J. D. Savee, A. M. Scheer, D. E. Shallcross, B. Rotavera, E. P. F. Lee, J. M. Dyke, D. K. W. Mok, D. L. Osborn, and C. J. Percival, *Science* **340**, 177 (2013).

[27] "Direct Kinetic Measurements of Criegee Intermediate (CH_2OO) Formed by Reaction of CH_2I with O_2," O. Welz, J. D. Savee, D. L. Osborn, S. S. Vasu, C. J. Percival, D. E. Shallcross, and C. A. Taatjes, *Science* **335**, 204 (2012).

[28] "Pressure-Dependent I-Atom Yield in the Reaction of CH_2I with O_2 Shows a Remarkable Apparent Third-Body Efficiency for O_2," H. Huang, A. J. Eskola, and C. A. Taatjes, *J. Phys. Chem. Lett.* **3**, 3399 (2012).

[29] "Direct Measurement of Criegee Intermediate (CH_2OO) Reactions with Acetone, Acetaldehyde, and Hexafluoroacetone," C. A. Taatjes, O. Welz, A. J. Eskola, J. D. Savee, D. L. Osborn, E. P. F. Lee, J. M. Dyke, D. W. K. Mok, D. E. Shallcross, and C. J. Percival, *Phys. Chem. Chem. Phys.* **14**, 10391 (2012).

[30] "Infrared Absorption Spectrum of the Simplest Criegee Intermediate CH_2OO," Y.-T. Su, Y.-H. Huang, H. A. Witek, and Y.-P. Lee, *Science* **340**, 174 (2013).

[31] "Ultraviolet Spectrum and Photochemistry of the Simplest Criegee Intermediate CH_2OO," J. M. Beames, F. Liu, L. Lu, and M. I. Lester, *J. Am. Chem. Soc.* **134**, 20045 (2012).

[32] "Communication: Determinaton of the Molecular Structure of the Simplest Criegee Intermediate CH2OO," M. Nakajima and Y. Endo, *J. Chem. Phys.* **139**, 101103 (2013).

[33] "Contribution to the Analysis of the $^3A_2 \leftarrow \tilde{X}^1A_1$ "Wulf" Transition of Ozone by High-Resolution Fourier Transform Spectrometry," A. J. Bouvier, D. Inard, V. Veyret, B. Bussery, R. Bacis, S. Churassy, J. Brion, J. Malicet, and R. H. Judge, *J. Mol. Spectrosc.* **190**, 189 (1998).

[34] "Characterization of a Metastable State of Ozone by High-Resolution Fourier Transform Spectrometry," A. J. Bouvier, R. bacis, B. Bussery, S. Churassy, D. Inard, M. Nota, J. Brion, J. Malicet, and S. M. Anderson, *Chem. Phys. Lett.* **255**, 263 (1996).

[35] "The Kinetics of the Nitrate Radical Self-Reaction," P. Biggs, C. E. Canosa-Mas, P. S. Monks, R. P. Wayne, T. Benter, and R. N. Schindler, *Int'l J. of Chemical Kinetics* **25**, 805 (1993).

[36] "The Nitrate Radical: Physics, Chemistry, and the Atmosphere," R. P. Wayne, I. Barnes, P. Biggs, J. P. Burrows, C. E. Canosa-Mas, J. Hjorth, G. L. Bras, G. K. Moortgat, D. Perner, G. Poulet, G. Restelli, and H. Sidebottom, *Atmos. Environ.* **25A**, 1 (1991).

[37] M. J. Frisch, G. W. Trucks, H. B. Schlegel, G. E. Scuseria, M. A. Robb, J. R. Cheeseman, G. Scalmani, V. Barone, B. Mennucci, G. A. Petersson, H. Nakatsuji, M. Caricato, X. Li, H. P. Hratchian, A. F. Izmaylov, J. Bloino, G. Zheng, J. L. Sonnenberg, M. Hada, M. Ehara, K. Toyota, R. Fukuda, J. Hasegawa, M. Ishida, T. Nakajima, Y. Honda, O. Kitao, H. Nakai, T. Vreven, J. A. Montgomery, Jr., J. E. Peralta, F. Ogliaro, M. Bearpark, J. J. Heyd, E. Brothers, K. N. Kudin, V. N. Staroverov, R. Kobayashi, J. Normand, K. Raghavachari, A. Rendell, J. C. Burant, S. S. Iyengar, J. Tomasi, M. Cossi, N. Rega, J. M. Millam, M. Klene, J. E. Knox, J. B. Cross, V. Bakken, C. Adamo, J. Jaramillo, R. Gomperts, R. E. Stratmann, O. Yazyev, A. J. Austin, R. Cammi, C. Pomelli, J. W. Ochterski, R. L. Martin, K. Morokuma, V. G. Zakrzewski, G. A. Voth, P. Salvador, J. J. Dannenberg, S. Dapprich, A. D. Daniels, Ö. Farkas, J. B. Foresman, J. V. Ortiz, J. Cioslowski, and D. J. Fox, "Gaussian 09 Revision A.1, gaussian Inc. Wallingford CT 2009.

[38] V. Mozhayskiy and A. Krylov, "ezSpectrum, http://iopenshell.usc.edu/downloads.

[39] "Measurement of the Absolute Absorption Cross Sections of the $\tilde{A} \leftarrow \tilde{X}$ Transition in Organic Peroxy Radicals by Dual Wavelength Cavity-Ringdown Spectroscopy," D. Melnik, R. Chhantyal-Pun, and T. A. Miller, *J. Phys. Chem. A* **114**, 11583 (2010).

[40] "The Electronic Transition Moment for the 0_0^0 Band of the $\tilde{A} - \tilde{X}$ Transition in the Ethyl Peroxy Radical," D. Melnik, P. S. Thomas, and T. A. Miller, *J. Phys. Chem. A* **115**, 13931 (2011).

[41] "Kinetic Measurements of the $C_2H_5O_2$ Radical Using Time-resolved CW-CRDS Spectroscopy with a Continuous Source," T. A. Miller and D. Melnik, *J. Chem. Phys.* **139**, 094201 (2013).

[42] "Cavity Ring-Down Spectroscopy of Quantitative Absorption Measurements," P. Zalicki and R. N. Zare, *J. Chem. Phys.* **102**, 2708 (1995).

[43] "Rotationally Resolved $\tilde{B} \leftarrow \tilde{X}$ Electronic Spectra of the Isopropoxy Radical: A Comparative Study," J. Liu, D. Melnik, and T. A. Miller, *J. Chem. Phys.* **139**, 094308 (2013).

[44] "Organic Peroxy Radicals: Kinetics, Spectroscopy and Tropospheric Chemistry," P. D. Lightfoot, R. A. Cox, J. N. Crowley, M. Destriau, G. D. Hayman, M. E. Jenkin, G. K. Moortgat, and F. Zabel, *Atmos. Envir.* **26A**, 1805 (1992).

[45] "Ultraviolet Absorption Cross Sections and Reaction Kinetics and Mechanisms for Peroxy Radicals in the Gas Phase," T. J. Wallington, P. Dagaut, and M. J. Kurylo, *Chem. Rev.* **92**, 667 (1992).

[46] "Gas-phase tropospheric chemistry of volatile organic compounds: 1. Alkanes and alkenes," R. Atkinson, *J. Phys. Chem. Ref. Data* **26**, 215 (1997).

[47] "The Ethylperoxy Radical: Its Ultraviolet Spectrum, Self-Reaction, and Reaction with HO_2, Each Studied as a Function of Temperature," F. F. Fenter, V. Catoire, R. Lesclaux, and P. D. Lightfoot, *J. Phys. Chem.* **97**, 3530 (1993).

[48] "Near-infrared kinetic spectroscopy of the HO_2 and $C_2H_5O_2$ self-reactions and cross-reactions," A. C. Noell, L. S. Alconcel, D. J. Robichaud, M. Okumura, and S. P. Sander, *J. Phys. Chem. A* **114**, 6983 (2010).

[49] "Chemical Kinetic Studies Using Ultraviolet Cavity Ring-Down Spectroscopic Detection: Self-Reaction of Ethyl and Ethylperoxy Radicals and the Reaction O_2+C_2H_5 →$C_2H_5O_2$," D. B. Atkinson and J. W. Hudgens, *J. Phys. Chem. A* **101**, 3901 (1997).

Appendix 1: Papers Acknowledging Support From This Grant

[1] "The $\tilde{A} - \tilde{X}$ Absorption of Vinoxy Radical Revisited: Normal and Herzberg-Teller Bands Observed Via Cavity Ringdown Spectroscopy," P. S. Thomas, R. Chhantyal-Pun, N. D. Kline, and T. A. Miller, *J. Chem. Phys.* **132**, 114302 (2010).

[2] "Cavity Ringdown Spectroscopy of the NIR $\tilde{A} - \tilde{X}$ Electronic Transition of Allyl Peroxy Radical (H_2C=CH-$CH_2OO\cdot$)," P. S. Thomas and T. A. Miller, *Chem. Phys. Lett.* **491**, 123 (2010).

[3] "Observation of the $\widetilde{A} - \widetilde{X}$ Electronic Transition of the β-Hydroxyethylperoxy Radical," R. Chhantyal-Pun, N. D. Kline, P. S. Thomas, and T. A. Miller, *J. Phys. Chem. Lett.* **1**, 1846 (2010).

[4] "Measurement of the Absolute Absorption Cross Sections of the $\tilde{A} \leftarrow \tilde{X}$ Transition in Organic Peroxy Radicals by Dual Wavelength Cavity-Ringdown Spectroscopy," D. Melnik, R. Chhantyal-Pun, and T. A. Miller, *J. Phys. Chem. A* **114**, 11583 (2010).

[5] "$\tilde{A} - \tilde{X}$ Absorption of Propargyl Peroxy (H-C=C-$CH_2OO\cdot$): A Cavity Ring-Down Spectroscopic and Computational Study," P. S. Thomas, N. D. Kline, and T. A. Miller, *J. Phys. Chem. A* **114**, 12437 (2010).

[6] "The $\tilde{A} - \tilde{X}$ Absorption of Cyclopentadienyl Peroxy Radical (c-$C_5H_5OO\cdot$): A Cavity Ringdown Spectroscopic and Computational Study," P. S. Thomas and T. A. Miller, *Chem. Phys. Letts.* **514**, 196 (2011).

[7] "The Electronic Transition Moment for the 0_0^0 Band of the $\tilde{A} - \tilde{X}$ Transition in the Ethyl Peroxy Radical," D. Melnik, P. S. Thomas, and T. A. Miller, *J. Phys. Chem. A* **115**, 13931 (2011).

[8] "Spectroscopic Studies of the $\tilde{A} - \tilde{X}$ Electronic Spectrum of the β-Hydroxyethylperoxy Radical: Structure and Dynamics," M.-W. Chen, G. M. P. Just, T. Codd, and T. A. Miller, *J. Chem. Phys.* **135**, 184304 (2011).

[9] "Analysis of the $\tilde{A} - \tilde{X}$ Electronic Tranistion of the 2,1-Hydroxypropylperoxy Radical Using Cavity Ringdown Spectroscopy," N. D. Kline and T. A. Miller, *Chem. Phys. Letts.* **530**, 16 (2012).

[10] "Detection and Characterization of Reactive Chemical Intermediates Using Cavity Ringdown Spectroscopy," N. Kline and T. A. Miller, in *Cavity Enhanced Spectroscopy and Sensing*, (Springer-Verlag, Berlin Heidelberg, 2014), p. Chapter 2.